

**COMPARISON OF THICK AND THIN SHELL THEORY RESULTS FOR BURIED  
ORTHOTROPIC CYLINDRICAL SHELL DUE TO INCIDENT SHEAR WAVE**

J.P. Dwivedi and V.P. Singh  
Department of Mechanical Engineering  
Institute of Technology  
Banaras Hindu University  
Varanasi 221 005

**ABSTRACT**

This paper deals with the comparison of thick and thin shell theories for buried orthotropic cylindrical shell excited by incident shear wave. For this purpose only axisymmetric response has been investigated and a perfect bond between the shell and surrounding medium has been assumed. The nature of variation of differences between the two shell theories results has been discussed for different soil conditions and angles of incidence of the shear wave. The differences in results as obtained by varying orthotropic parameters have been compared with the changes in the results of thick and thin shell theories. It is realized that shell response is significantly influenced by variation in the values of the orthotropic parameters rather than the choice of shell model.

**INTRODUCTION**

Some papers [1,2,3,4] have appeared in the past where attempts have been made to compare the response of a cylindrical shell as obtained from thick and thin shell theories. However, in these papers results are not presented for buried shells. In a paper, Chonan [5] has discussed the differences between the results of thick and thin shell theories for buried cylindrical shell subjected to a moving load. The main emphasis of this paper has been on the effect of imperfect bond on the radial displacement of the shell for a constant surrounding soil parameter. In this paper only radial displacements have been compared, whereas it has been reported [6] that the large axial displacement is the most frequent cause of failure of buried pipelines. In an earlier paper [7] authors have compared the thick and thin shell theory results for buried orthotropic cylindrical shell. In this work, however, results have been presented for the case of incident plane longitudinal wave. To the best of authors' knowledge there appears to be no work available giving the comparison of thick and thin shell theories results for buried orthotropic cylindrical shell subjected to shear wave travelling in surrounding infinite medium.

The aim of this paper, therefore, is to compare the responses of buried orthotropic thick and thin cylindrical shells due to shear wave excitation under different soil conditions and for different angles of incidence. The main purpose is to study the nature of variation of qualitative as well as quantitative difference between the two shell theory results as the rigidity of surrounding ground is changed. The changes in the results due to variation of orthotropy parameters have been compared with the differences in the results of thick and thin shell theories. It is found that variation in orthotropy parameters

produce significant changes in the results ; compared to this, no prominent change in shell response is observed when the choice is changed from a thick to thin shell approximation.

### GOVERNING EQUATIONS AND FORMULATION

Reference [8] presents a detailed and step-wise formulation of the problem of dynamic response of buried orthotropic cylindrical shell subjected to a longitudinal wave moving in a linearly elastic, homogeneous and isotropic infinite medium along axis of the shell. Therefore, this paper includes only those descriptions and equations which appear to be necessary for the sake of completeness.

### THICK SHELL EQUATIONS

A thick shell model including the effect of shear deformation and rotary inertia is considered. To describe the shell geometry a cylindrical polar co-ordinate system  $(r, \theta, x)$  is defined such that  $x$  coincides with the axis of the shell. The stress-strain relations for the shell material were assumed to be of the form.

$$\begin{aligned}\sigma_{xx} &= E_{x1} \epsilon_{xx} + E_{\nu 1} \epsilon_{\theta\theta} \\ \sigma_{\theta\theta} &= E_{\nu 1} \epsilon_{xx} + E_{\theta 1} \epsilon_{\theta\theta} \\ \sigma_{xr} &= G_{x1} 2 \epsilon_{xr}\end{aligned}\quad (1)$$

with  $E_{x1}$ ,  $E_{\theta 1}$ ,  $E_{\nu 1}$  and  $G_{x1}$  as the four independent moduli.

The shell with mean radius  $R$ , thickness  $h$  and density  $\rho_0$  is subjected to a shear wave of wavelength  $\Delta$  ( $=2\pi/\xi$ ) and speed  $c$  ( $=\omega/\xi$ ) moving along the axis of the shell. The boundary conditions and equations of motion of the shell are taken to be the same as in Ref. [8], then, by following the procedure detailed in Ref. [8], the final shell response equation are obtained in matrix form,

$$[A] \{M\} = \{F\} \quad (2)$$

$$\text{where } \{M\} = \left[ \bar{U}, \bar{V}, \bar{W}, \frac{B_2}{Rd_0}, \frac{B_4}{Rd_0} \right]^T; \bar{U} = \bar{u}/d_0, \bar{V} = h\bar{\phi}_x/2d_0, \bar{W} = \bar{w}/d_0$$

and  $B_2$  and  $B_4$  are arbitrary constants.  $d_0$  is a constant depending on the intensity of incident shear wave, and having the dimension of length. The terms of matrices  $[A]$  and  $\{F\}$  are defined as follows :

$$\begin{aligned}A_{11} &= -1\beta\bar{h}n_2/n_3; A_{12} = 2ik^2\beta; A_{13} = -\bar{h} \left[ \left( 1 + \frac{\bar{h}^2}{12} \right) \eta_1/\eta_3 + \beta^2k^2 \right] + \Omega^2 \\ A_{14} &= \left[ 1 + \frac{\bar{h}}{2} \right] \bar{\mu} \left[ \tau^2 \gamma^2 \left\{ K_0 \left( \alpha_1 \right) + \frac{K_1 \left( \alpha_1 \right)}{\alpha_1} \right\} - \frac{(\tau^2 - 2) \gamma^2}{\alpha_1} K_1 \left( \alpha_1 \right) \right. \\ &\quad \left. - \beta^2 (\tau^2 - 2) K_0 \left( \alpha_1 \right) \right];\end{aligned}$$

$$A_{15} = \left[ 1 + \frac{\bar{h}}{2} \right] \bar{\mu} \left[ 1 \tau^2 \beta \delta \left\{ K_0 (\alpha_2) + \frac{\gamma K_1^2 (\alpha_2)}{\alpha_1} \right\} - \frac{1\beta\gamma (\tau - 2)}{\alpha_1} K_1 (\alpha_2) - 1\beta\delta (\tau^2 - 2) K_0 (\alpha_2) \right];$$

$$A_{21} = \frac{\bar{h}^2}{12} \left[ \Omega^2 - \frac{\bar{h} \beta^2}{\eta_3} \right]; \quad A_{22} = \left[ -\frac{\bar{h} \beta^2}{6 \eta_3} - 2k^2 + \frac{\bar{h}}{6} + \Omega^2 \right];$$

$$A_{23} = -1\beta\delta k^2; \quad A_{24} = \bar{h} \left[ 1 + \frac{\bar{h}}{2} \right] \bar{\mu} \left[ -1\beta\gamma K_1 (\alpha_1) \right];$$

$$A_{25} = \frac{\bar{h}}{2} \left[ 1 + \frac{\bar{h}}{2} \right] \bar{\mu} \left[ (\beta^2 + \delta^2) K_1 (\alpha_2) \right]; \quad A_{31} = -\frac{\bar{h} \beta^2}{\eta_3} + \Omega^2;$$

$$A_{32} = \frac{\bar{h}}{6} \quad A_{31}; \quad A_{33} = -A_{11}; \quad A_{34} = \left[ 1 + \frac{\bar{h}}{2} \right] \bar{\mu} \left[ -21\beta\gamma K_1 (\alpha_1) \right];$$

$$A_{35} = 2/\bar{h} \quad A_{25}; \quad A_{41} = A_{42} = 1; \quad A_{43} = 0; \quad A_{44} = -1\beta K_0 (\alpha_1)$$

$$A_{45} = \delta K_0 (\alpha_2); \quad A_{51} = A_{52} = 0; \quad A_{53} = 1; \quad A_{54} = \gamma K_1 (\alpha_1);$$

$$A_{55} = 1\beta K_1 (\alpha_2);$$

$$F_1 = - \left[ 1 + \frac{\bar{h}}{2} \right] 2\bar{\mu}1\beta \left\{ \frac{I_1 (\alpha_2)}{1 + \frac{\bar{h}}{2}} - \delta I_0 (\alpha_2) \right\};$$

$$F_2 = - \left[ 1 + \frac{\bar{h}}{2} \right] \bar{\mu} \frac{\bar{h}}{2} \left[ \beta^2 + \delta^2 \right] I_1 (\alpha_2);$$

$$F_3 = - \left[ 1 + \frac{\bar{h}}{2} \right] \bar{\mu} \left[ \beta^2 + \delta^2 \right] I_1 (\alpha_2); \quad F_4 = \delta I_0 (\alpha_2)$$

$$F_5 = -1\beta I_1 (\alpha_2);$$

(3)

Here,  $\eta_1 = E_{\theta 1}/E_{x1}$ ,  $\eta_2 = E_{\nu 1}/E_{x1}$  and  $\eta_3 = G_{x1}/E_{x1}$  are the non-dimensionalized orthotropy parameters of the shell in which  $E_{x1}$ ,  $E_{\theta 1}$ ,  $E_{\nu 1}$  and  $G_{x1}$  are four independent moduli; and

$\Omega^2 = (\rho_0 h R / G_{x1}) \omega^2 = \beta^2 \bar{h} \bar{c}^2 \tau^2 \bar{\rho} \bar{\mu}$  is the non-dimensional frequency of the shell;  $\bar{\rho} = \rho_0 / \rho_m$  and  $\bar{\mu} = \mu / G_{x1}$  are, respectively, density of the

surrounding soil and the modulus of rigidity measured in terms of the corresponding values for the shell material. In the case of the shear wave moving at an angle  $\phi$  with the axis of the shell, the apparent wave speed along the shell axis will be  $c$  ( $= c_2/\cos\phi$ ). The value of non-dimensional apparent wave speed,  $\bar{c}$  ( $=c/c_2$ ), therefore, will always be greater than 1.0. Other quantities in matrix coefficients are defined as follows :

$$\alpha_1 = (1 + \bar{h}/2)\gamma, \quad \gamma = \beta \sqrt{1 - (c/c_1)^2}, \quad \alpha_2 = (1 + \bar{h}/2)\delta$$

$$\delta = \beta \sqrt{1 - (c/c_2)^2};$$

$$\beta = \xi R = 2\pi R/\Lambda; \quad \bar{h} = h/R; \quad \tau^2 = c_1^2/c_2^2 = 2(1 - \nu_m)/(1 - 2\nu_m) \quad (4)$$

where  $\nu_m$  is the Poisson's ratio of the medium, and  $k$  is the shear correction factor ( $= \pi/\sqrt{12}$ ).  $c_1 = \left\{ (\lambda + 2\mu)/\rho_m \right\}^{1/2}$  and  $c_2 = \left\{ \mu/\rho_m \right\}^{1/2}$  are, respectively, the speeds of propagation of the longitudinal and shear waves in the surrounding medium.  $\lambda$  and  $\mu$  are the Lamé's constants, and  $\rho_m$  is the density of the medium.  $I_n$  and  $K_n$  ( $n = 0, 1$ ) are the modified Bessel functions of first and second kinds and as their arguments are imaginary they will be transformed to  $J_n$  and  $Y_n$ , respectively.

The matrix  $\{M\}$ , in equation (2), contains  $\bar{U}$ ,  $\bar{V}$  and  $\bar{W}$ , which are the non-dimensionalized deformation amplitudes of the middle surface of the shell in the axial, tangential and radial directions, respectively.

#### THIN SHELL EQUATIONS

With similar geometrical coordinates and notations for description of different quantities, and by following the procedure and the steps as discussed above for thick shell model, the final response equation for the thin shell can similarly be expressed as.

$$[A] \{M\} = \{F\} \quad (5)$$

where  $\{M\} = \left[ \bar{U}, \bar{W}, \frac{B_2}{Rd_0}, \frac{B_4}{Rd_0} \right]^T$  and elements of matrices  $[A]$  and

$\{F\}$  are as follows :

$$A'_{11} = \frac{\bar{h}\beta}{\eta_3} \left[ \eta_2 + \frac{\bar{h}^2 \beta^2}{12} \right], \quad A'_{12} = \frac{\bar{h} \eta_1}{12} \left[ 12 + \bar{h}^2 + \bar{h}^2 \beta^4/\eta_1 \right] - \Omega^2,$$

$$A'_{13} = -A'_{14}, \quad A'_{14} = -A'_{15}, \quad A'_{21} = A'_{31}, \quad A'_{22} = A'_{11},$$

$$\begin{aligned}
 A'_{23} &= \frac{2}{\bar{h}} A_{24}, A'_{24} = \frac{2}{\bar{h}} A_{25}, A'_{31} = 1, A'_{32} = 0, A'_{33} = A_{44}, \\
 A'_{34} &= A_{45}, A'_{41} = 0, A'_{42} = 1, A'_{43} = A_{54}, A'_{44} = A_{55}, \\
 F'_1 &= -F_1, F'_2 = \frac{2}{\bar{h}} F_2, F'_3 = F_4, F'_4 = F_5, \\
 \{M'\} &= \left[ \bar{U}, \bar{Q}, \frac{B_2}{Rd_o}, \frac{B_4}{Rd_o} \right]^T = \left[ \frac{\bar{u}}{d_o}, \frac{\bar{w}}{d_o}, \frac{B_2}{Rd_o}, \frac{B_4}{Rd_o} \right]^T \quad (6)
 \end{aligned}$$

The orthotropic parameters  $\eta_1$ ,  $\eta_2$  and  $\eta_3$  are the same as defined in the previous section.

### RESULTS AND DISCUSSION

The main emphasis of this paper is to highlight the difference in shell deformation as obtained by using thick and thin shell theories. Another important aspect is to compare the difference in results due to variation of orthotropy parameter with changes in results as obtained from thick and thin shell theories. Shell deformation amplitudes in radial and axial directions have been written in a non-dimensionalized form. Results have been plotted against the non-dimensionalized wavelength parameter  $\beta$  ( $= 2\pi R/\lambda$ ) of the incident wave for different angles of incidence  $\phi$  ( $= 5^\circ, 80^\circ$ ) and various ground conditions. A nearly grazing angle of incidence is represented by  $\phi = 5^\circ$  and  $80^\circ$  represents a general striking angle of the wave. Variation of  $\beta$  from 0.0 to 1.0 is expected to cover the practical range of pipe radius and wavelength of shear wave.

The non-dimensionalized shell orthotropy parameters  $\eta_1$ ,  $\eta_2$  and  $\eta_3$  are varied over a wide range which are expected to cover a large group of composite materials. Different values of  $\eta_1$ ,  $\eta_2$  and  $\eta_3$  are:  $\eta_1 = 0.05, 0.50, 1.0$ ;  $\eta_2 = 0.005, 0.05, 0.10$  and  $\eta_3 = 0.01, 0.02, 0.20$ . With the variation of one parameter the other two are kept constant. To account for different kinds of ground conditions the parameter  $\bar{\mu}$  is varied between 0.01 to 10.0.  $\bar{\mu} = 0.01$  represents very soft surrounding soil, whereas,  $\bar{\mu} = 10.0$  represents very hard and rocky soil. The value of different parameters have been kept constant as:  $\bar{h} = 0.10$ ,  $\bar{\rho} = 0.30$  and  $\nu_m = 0.25$ .

Figures 1, 2 and 3 show the results for a nearly grazing angle of incidence ( $\phi = 5^\circ$ ) wherein, respectively,  $\eta_1$ ,  $\eta_2$  and  $\eta_3$  have been taken as parameters. Results have been included for  $\bar{\mu} = 0.01$  as the choice of shell model does not make any difference in axial displacement. It is seen from Figures (1-3) that the axial displacement of pipe surrounded by soft soil ( $\bar{\mu} = 0.1$ ) yields almost the same result for both the shell

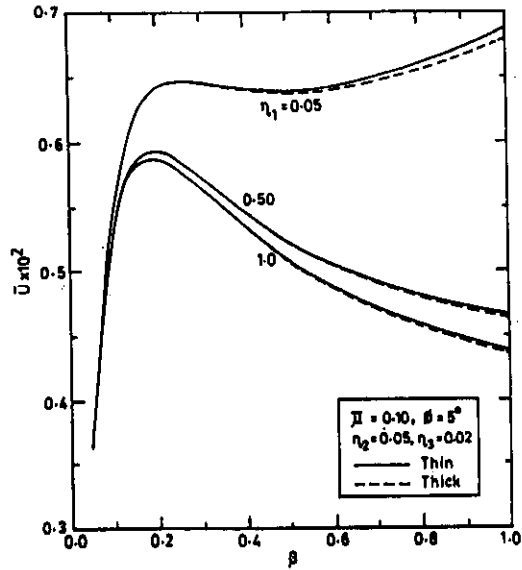


Fig. 1 Axial displacement ( $\bar{U}$ ) versus wavelength parameter ( $\beta$ ) for  $\bar{\mu} = 0.1$  and  $\phi = 5^\circ$  with  $\eta_1$  as parameter.

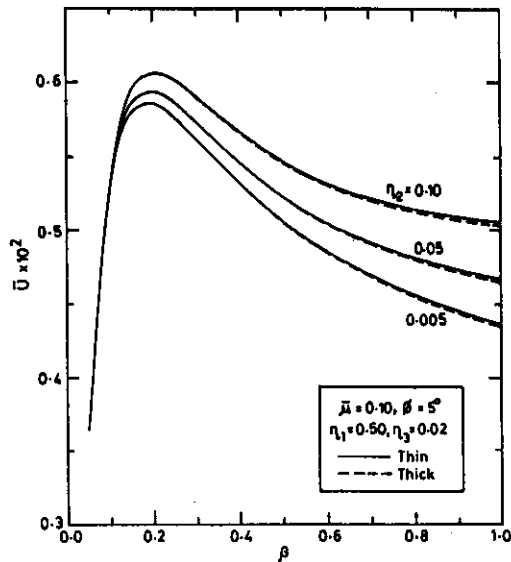


Fig. 2 Axial displacement ( $\bar{U}$ ) versus wavelength parameter ( $\beta$ ) for  $\bar{\mu} = 0.1$  and  $\phi = 5^\circ$  with  $\eta_2$  as parameter.

models except for a very little difference when  $\eta_1 = 0.05$ . The two shell theories give exactly the same axial displacement when  $\eta_3$  is varied, as shown in Figure 3. The values of  $\bar{U}$  are largely affected as orthotropy parameters  $\eta_1, \eta_2$  and  $\eta_3$  are varied. Although it is not shown through Figures but change in shell model does not bring any differences in  $\bar{U}$  when angles of incidence is increased to  $80^\circ$ . It is observed that in soft surrounding soil ( $\bar{\mu} = 0.10$ ) the choice of the shell model does not produce any significant difference in axial displacement, irrespective of angle of incidence. However, the changes in  $\bar{U}$  due to variation of orthotropy parameters  $\eta_1, \eta_2$  and  $\eta_3$  can not be overlooked.

In Figures 4-7, the axial displacement  $\bar{U}$  of the shell has been shown at higher angle of incidence ( $\phi = 80^\circ$ ). For grazing angle of incidence no difference in result due to change of shell model was visible at  $\bar{\mu} = 1.0$  or  $10.0$ .

When rigidity of the shell is comparable to that of the ground, the results are shown in Figures 4 and 5 for variation of  $\eta_1$  and  $\eta_2$ , respectively. Figure 4 shows that a little difference between the predictions of the thin and thick shell theories are observed at smaller wavelength and  $\bar{U}$  is more with thin shell theory approximation. However, the changes in orthotropy parameter  $\eta_1$  have no influence on  $\bar{U}$ . It is not shown but same is found to be true with the variation of  $\eta_2$ . Variation in the values of orthotropy parameter  $\eta_3$  influences the axial deformation as evidenced from Figure 5. At the same time the difference in results due to change in shell model cannot be overlooked. This difference appears to be augmented with decreasing value of  $\eta_3$ . In general, for medium hard soil ( $\bar{\mu} = 1.0$ ) difference in results due to choice of the shell model exist for larger angle of incidence and  $\bar{U}$  is always higher with thin shell theory assumption.

For very hard and rocky surrounding soil ( $\bar{\mu} = 10.0$ ) results are shown in Figures 6 and 7. Differences in  $\bar{U}$  are observed as shell model is changed from thin to thick. Result has been shown for  $\eta_2$  (Figure 6), however, similar trend is observed with  $\eta_1$  as orthotropy parameter (not shown through Figures). Variation in  $\eta_3$  does not show any changes in axial displacement of thin shell as Figure 7 indicates. But with thick shell model  $\bar{U}$  increases with increasing value of orthotropy parameter  $\eta_3$ . The differences between the predictions of the thin and thick shell theories appear to be increasing with increasing value of  $\beta$ . Unlike Figures 1-5, with the thick shell model the axial displacement is augmented when surrounding soil is very hard and rocky. It is concluded that when rigidity of the ground is more than the rigidity of the shell, the thick and thin shell theories indicate an appreciable difference in

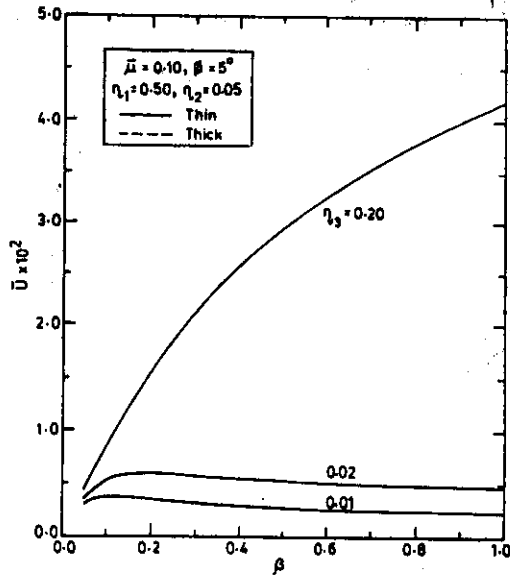


Fig. 3 Axial displacement ( $\bar{U}$ ) versus wavelength parameter ( $\beta$ ) for  $\bar{\mu} = 0.1$  and  $\phi = 5^\circ$  with  $\eta_3$  as parameter.

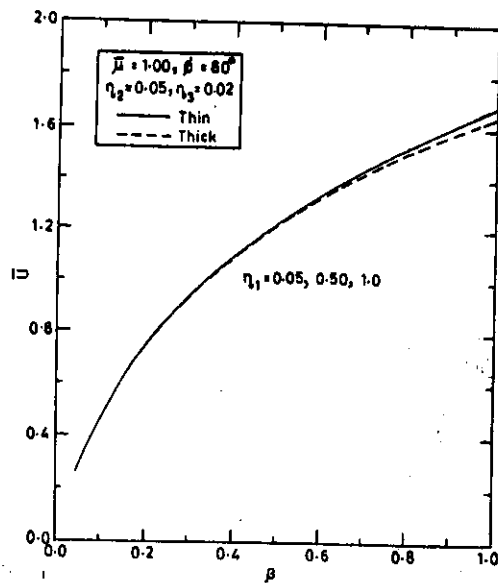


Fig. 4 Axial displacement ( $\bar{U}$ ) versus wavelength parameter ( $\beta$ ) for  $\bar{\mu} = 1.0$  and  $\phi = 80^\circ$  with  $\eta_1$  as parameter.



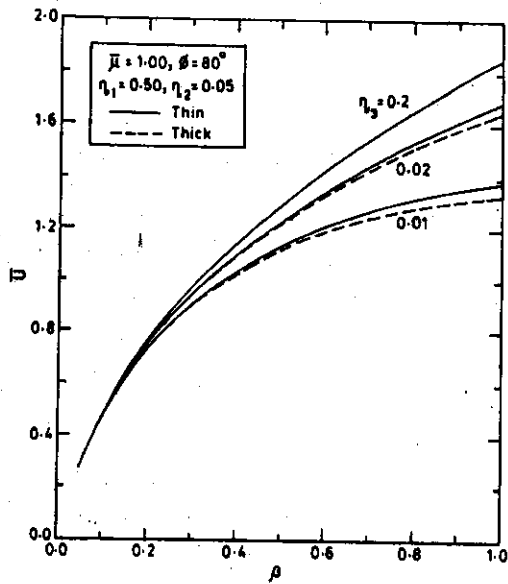


Fig. 5 Axial displacement ( $\bar{U}$ ) versus wavelength parameter ( $\beta$ ) for  $\bar{\mu} = 1$  and  $\phi = 80^\circ$  with  $\eta_3$  as parameter.

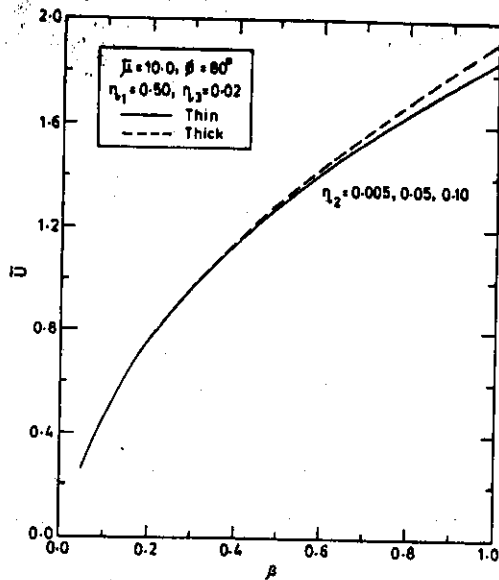


Fig. 6 Axial displacement ( $\bar{U}$ ) versus wavelength parameter ( $\beta$ ) for  $\bar{\mu} = 10.0$  and  $\phi = 80^\circ$  with  $\eta_2$  as parameter.

$\bar{U}$  with higher value for thick shell, when wave strikes the shell at higher angle of incidence.

Figures 8 to 10 show the variations of radial displacement  $\bar{W}$  with wavelength parameter  $\beta (= 2\pi R/\lambda)$ .

Figures 8 and 9 show the results for a nearly grazing angle of incidence in a very soft and sandy surrounding soil ( $\bar{\mu} = 0.01$ ). Both the shell models give the same value of  $\bar{W}$  except for a very little change at  $\eta_1 = 0.05$  (Figure 8). But changes in orthotropy parameter  $\eta_1$  produces a significant difference in  $\bar{W}$  for both the thin and thick shells. Similar behaviour is observed at higher angle of incidence (not shown through figures). Figure 9 shows that the difference in radial displacement  $\bar{W}$  for two shell models is almost comparable to the difference in result as obtained of  $\eta_2$ . A similar trend is observed when angle of incidence is changed to  $80^\circ$ . The result for  $\bar{W}$  due to changes in  $\eta_3$  for the two shell models emerges out with the same conclusion as drawn in favour of  $\eta_1$ . In fact though it is not shown in figures, for  $\bar{\mu} = 0.10$  the radial displacement due to change of orthotropy parameters  $\eta_1$ ,  $\eta_2$  and  $\eta_3$  for the two shell theories shows similar trend observed with  $\bar{\mu} = 0.01$ .

Figure 10 shows the result at  $\bar{\mu} = 1.0$  for  $\phi = 5^\circ$ . It is evident from the figure that difference in  $\bar{W}$  is much more significant due to changes in orthotropy parameter rather than the choice of shell model. It is not shown but variation in  $\eta_2$  or  $\eta_3$  give almost the same values of  $\bar{W}$  with both the shell models. The results obtained for very hard and rocky surrounding soil did not show any difference between the predictions of thick and thin shell theories, therefore, corresponding plots have not been included.

### CONCLUSIONS

On the basis of result presented following conclusions can be drawn :

1. For smaller angle of incidence the axial displacements are hardly affected due to change of shell model.
2. In a softer medium ( $\bar{\mu} < 0.10$ ), the same axial displacement is obtained from both the shell models ; but variations in orthotropy parameters ( $\eta_1$ ,  $\eta_2$  and  $\eta_3$ ) produce significant changes in axial displacement.
3. For hard surrounding soil ( $\bar{\mu} \geq 1.0$ ) the difference in  $\bar{U}$ , as obtained from thick and thin shell theories, are clearly visible ; compared to this, changes in  $\eta_1$  and  $\eta_2$  do not produce any difference at all in the axial displacement. However the axial displacement changes with variation in the value of  $\eta_3$ .

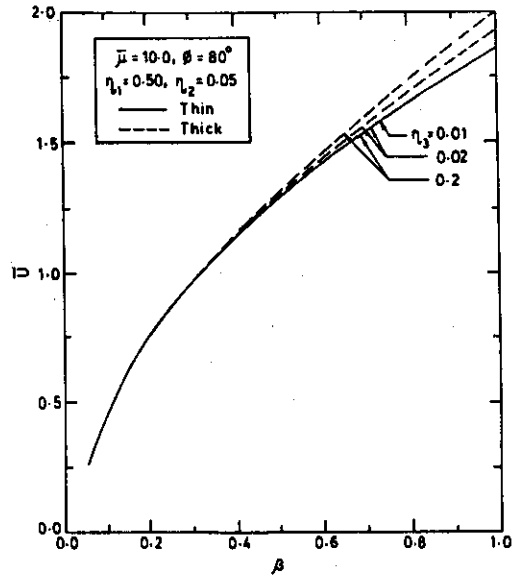


Fig. 7 Axial displacement ( $\bar{U}$ ) versus wavelength parameter ( $\beta$ ) for  $\bar{\mu} = 10.0$  and  $\phi = 80^\circ$  with  $\eta_3$  as parameter.

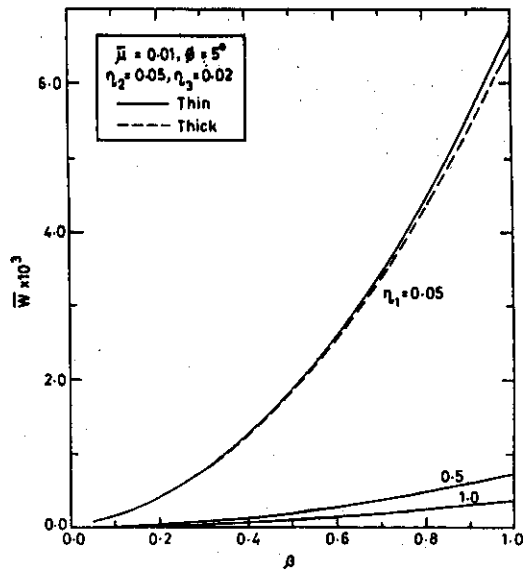


Fig. 8 Radial displacement ( $\bar{W}$ ) versus wavelength parameter ( $\beta$ ) for  $\bar{\mu} = 0.01$  and  $\phi = 5^\circ$  with  $\eta_1$  as parameter.

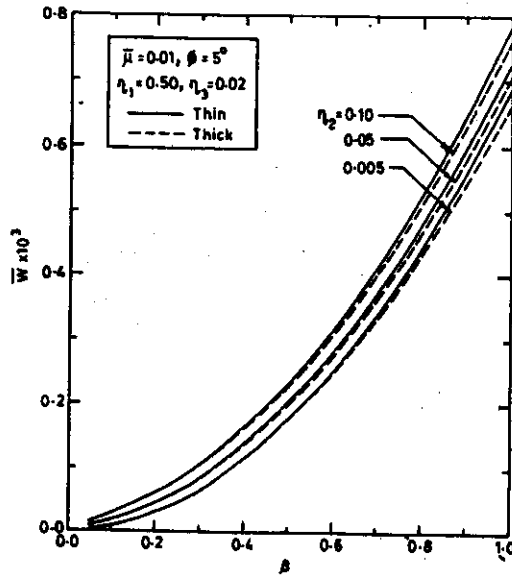


Fig. 9 Radial displacement ( $\bar{W}$ ) versus wavelength parameter ( $\beta$ ) for  $\bar{\mu} = 0.01$  and  $\phi = 5^\circ$  with  $\eta_2$  as parameter.

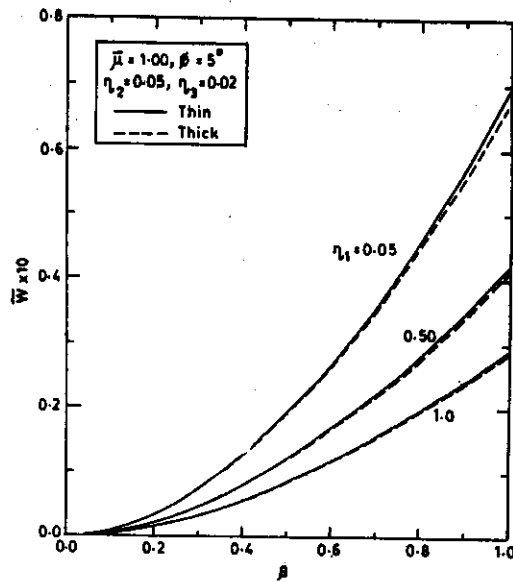


Fig. 10 Radial displacement ( $\bar{W}$ ) versus wavelength parameter ( $\beta$ ) for  $\bar{\mu} = 1.0$  and  $\phi = 5^\circ$  with  $\eta_1$  as parameter.

4. The choice of shell model makes little difference in radial displacements which is observed only when surrounding medium is very soft and sandy. But variations in  $\eta_1$ ,  $\eta_2$  and  $\eta_3$  show remarkable changes in radial displacement under all soil conditions.
5. For larger wavelength ( $\beta < 0.40$ ) displacement (axial or radial) are not dependent of shell model.

#### REFERENCES

1. Chonan, S. (1981). Moving load on a two layered cylindrical shell with imperfect bonding. J. Acoust. Soc. Am., 69, 1015-1020.
2. Suzuki, S. (1979). Dynamic behaviour of thin cylindrical shells subjected to transient inner pressures-effects of shearing force and rotatory inertia. Nuclear Engg. Design., 51, 423-429.
3. Chonan, S. (1977). Response of a fluid-filled cylindrical shell to a moving load. J. Sound. & Vib., 55, 419-430.
4. Chonan, S. (1984). Response of a pre-stressed, orthotropic thick cylindrical shell subjected to a pressure pulse. J. Sound. & Vib., 93, 31-38.
5. Chonan, S. (1981). Dynamic response of a cylindrical shell imperfectly bounded to a surrounding continuum of infinite extent. J. Sound & Vib., 78, 257-267.
6. Hindy, A and Novak, M. (1979). Earthquake response of underground pipelines. Int. J. Earth. Engg. Struct. Dyn., 7, 451-476.
7. Singh, V.P., Upadhyay, P.C. and Kishor, B. (1987). A comparison of thick and thin shell theory results for buried orthotropic cylindrical shells. J. Sound & Vib., 119, 339-345.
8. Singh, V.P., Upadhyay, P.C. and Kishor, B. (1987). On the dynamic response of buried orthotropic cylindrical shells. J. Sound & Vib., 113, 101-115.

#### NOMENCLATURE

[A] {A'}	matrices defined in equations 1 and 4, respectively
$B_2$ and $B_1$	arbitrary constants
c	apparent wave speed along the shell axis
$c_1$	longitudinal wave speed in the surrounding medium
$c_2$	shear wave speed in the surrounding medium
$d_0$	a constant depending upon the intensity of incident S-wave and having the dimension of length
$E_{x1}, E_{\theta 1}, E_{\nu 1}$	elastic moduli of the shell material
{F}, {F'}	column matrices defined in equations (1) & (4) respectively
$G_{x1}$	shear modulus of the shell material
h	thickness of the shell
$\bar{h} = h/R$	non-dimensional thickness of the shell

$I_n$	modified Bessel function of first kind
$K_n$	modified Bessel function of second kind
$K$	shear correction factor
$\{M\}$ and $\{M'\}$	column matrices defined in equations (1) & (4) respectively
$R$	mean radius of the shell
$r$	radial coordinate
$t$	time
$\bar{U}$	non-dimensional displacement of the middle surface of the shell in axial direction
$\bar{u}$	displacement amplitude of the shell middle surface in the axial direction
$\bar{W}$	non-dimensional displacement of the middle surface of the shell in radial direction
$\bar{w}$	displacement amplitude of the middle surface of the shell in radial direction
$x$	co-ordinate along the shell axis
$\alpha_1$ and $\alpha_2$	defined in equation (3)
$\nu, \delta$	defined in equation (3)
$\eta_1, \eta_2, \eta_3$	non-dimensional orthotropy parameters of the shell
$\theta$	tangential co-ordinate
$\Lambda$	wavelength of the incident wave
$\lambda$ & $\mu$	Lame's constants
$\bar{\mu}$	non-dimensional modulus of rigidity of the soil
$\nu_m$	Poisson's ratio of the soil medium
$\xi$ ( $=\omega/c$ )	apparent wave number
$\rho_0$	density of the shell material
$\rho_m$	density of the medium
$\bar{\rho}$	density ratio of the shell to the medium
$\tau^2 \left\{ = \left[ c_1^2 / c_2^2 \right] \right\}$	defined for equation (2)
$\phi$	angle of wave incidence
$\Omega^2$	non-dimensional frequency of the shell
$\omega$	circular frequency

**Subscripts**

$m$	medium
$\theta$	tangential direction

## DAMAGE REPORT OF THE LATUR - OSMANABAD EARTHQUAKE OF SEPTEMBER 30, 1993

A. Sinvhal, P.R. Bose and R.N. Dubey  
Department of Earthquake Engineering,  
University of Roorkee,  
Roorkee, U.P., India, 247667.

### ABSTRACT

Widespread devastation and loss of life were witnessed in the epicentral region of the September 30, 1993 earthquake in the 2 districts of Latur and Osmanabad in south eastern Maharashtra. Traditional construction in the region was non-engineered and had no resistance against horizontal earthquake forces. In most houses walls were made of random rubble stone masonry and such structures suffered extensive damage. Survey of various earthquake affected villages, engineered and non-engineered buildings, hospitals, forts and monuments, places of worship, schools, building materials used, construction practice prevalent in the region, their performance, causes of high casualty figures and strange phenomena associated with the earthquake are presented in this paper.

### INTRODUCTION

The ten day long Ganesh festival concluded with the immersion of idols in a finale that lasted well into the night of September 29, 1993. Tired after the prolonged festivities the villagers of Killari slept, unaware of the impending doom. The entire Marathwada region was shaken up violently by an earthquake of magnitude 6.4, at 3.56 a.m. IST, (- 5.5 hours for GMT), on 30th September, 1993, on the Maharashtra-Karnataka border. Milder tremors followed in quick succession at 4.41 a.m., 6.24 a.m. 6.34 a.m. and 7.48 a.m.

Sholapur is the biggest town nearest to the devastated region. People were jolted out of their sleep in the states of Maharashtra, Karnataka, Andhra Pradesh, Tamil Nadu, Gujarat and Madhya Pradesh. The earthquake was felt with ferocity in the towns of Gulbarga, Bijapur, Bidar and Raichur. A mild tremor was also felt in Dharwad, Bellary and Belgaum districts. Most of the worst affected villages in Karnataka lie along the Bhima river which runs through the four northern districts of Karnataka.

More than 50 villages within an area of 100 square km on both sides of Terna River were severely affected. This river forms a natural divide between Latur and Osmanabad districts in the region ravaged by the quake. Killari, a densely populated and prosperous village 45 km south of Latur in Ausa taluka, was one of the worst affected villages and also the epicentre, 76° 35'E, 18° 03'N. A 15 km segment stretching between Makni dam and Killari bore the brunt of the devastation. Not a single stone structure in these villages was left intact and not a single family was left unscathed. The worst affected villages were Ekondi, Ganjankheda, Gubal, Huli, Kawtha, Killari, Killariwadi, Lamjana, Limbada, Mangrul, Peth Sangvi, Rajegaon, Sastur, Tausigarh, Talni, etc., shown in fig 1.

Visiting damaged and quake affected areas for study purposes is not simple and creates tremendous hardships. The stench of rotting flesh still buried under the debris was mixed with the nauseating smell and sight of numerous cremations. The silent and morbid atmosphere was pierced occasionally by hysterical wailing of villagers. As wood was in short supply broken door frames and wooden rafters were used for on the spot cremations. This, coupled with unseasonal rain made the survey work difficult and could be completed only because of great determination, courage and steadfastness on the part of authors. The rescue and relief work carried out by several agencies working in the area was hampered by movement of VIPs, idle onlookers and rain. This led the Army to seal off the area.